



HAL
open science

Femtosecond laser filamentation and applications

Aurélien Houard, André Mysyrowicz

► **To cite this version:**

Aurélien Houard, André Mysyrowicz. Femtosecond laser filamentation and applications. Light Filaments: Structures, challenges and applications, Institution of Engineering and Technology, pp.11-30, 2021, 10.1049/SBEW527E_ch1 . hal-03600581

HAL Id: hal-03600581

<https://ensta-paris.hal.science/hal-03600581>

Submitted on 4 Apr 2022

HAL is a multi-disciplinary open access archive for the deposit and dissemination of scientific research documents, whether they are published or not. The documents may come from teaching and research institutions in France or abroad, or from public or private research centers.

L'archive ouverte pluridisciplinaire **HAL**, est destinée au dépôt et à la diffusion de documents scientifiques de niveau recherche, publiés ou non, émanant des établissements d'enseignement et de recherche français ou étrangers, des laboratoires publics ou privés.

Femtosecond laser filamentation and applications

Aurélien Houard¹, André Mysyrowicz¹

Femtosecond filamentation is a spectacular phenomenon whereby a short laser pulse propagates nonlinearly through a transparent medium allowing high peak light intensities to be transferred over distances far exceeding the beam Rayleigh length, as if diffraction were suppressed. In this chapter, after a brief description of some key features of filamentation, we put the accent upon some potential applications.

1.1. Basic concepts

The filamentation process is initiated by the optical Kerr effect, responsible for a light intensity dependent index of refraction. A positive self-induced change of refractive index, even if minute, is cumulative upon propagation and leads to beam self-focusing. Self-focusing overcomes diffraction provided the initial power of the pulse exceeds a critical value P_{cr} [1]. In air, P_{cr} is a few GW for a pulse at 800 nm of 50 fs duration corresponding to a few mJ of pulse energy (in a transparent solid such a fused silica, a few μJ are sufficient). Upon further propagation, the peak intensity becomes high enough to ionize air molecules in a multiphoton process. Beam collapse is then arrested by high field ionization and the defocusing effect of the ensuing plasma. A complex behaviour emerges, where diffraction, group velocity dispersion, optical Kerr effect, absorption due to ionization, space-time focusing, pulse self-steepening, plasma defocusing and plasma reabsorption all contribute. A filament core surrounded and replenished by a reservoir of photons bath is emerging, as shown in Figure 1.1 showing the calculated propagation of a laser pulse centred at 800 nm with initial power $P \sim P_{cr}$.

¹Laboratoire d'Optique Appliquée, ENSTA Paris, CNRS, Ecole Polytechnique, Institut Polytechnique de Paris, Palaiseau, France.

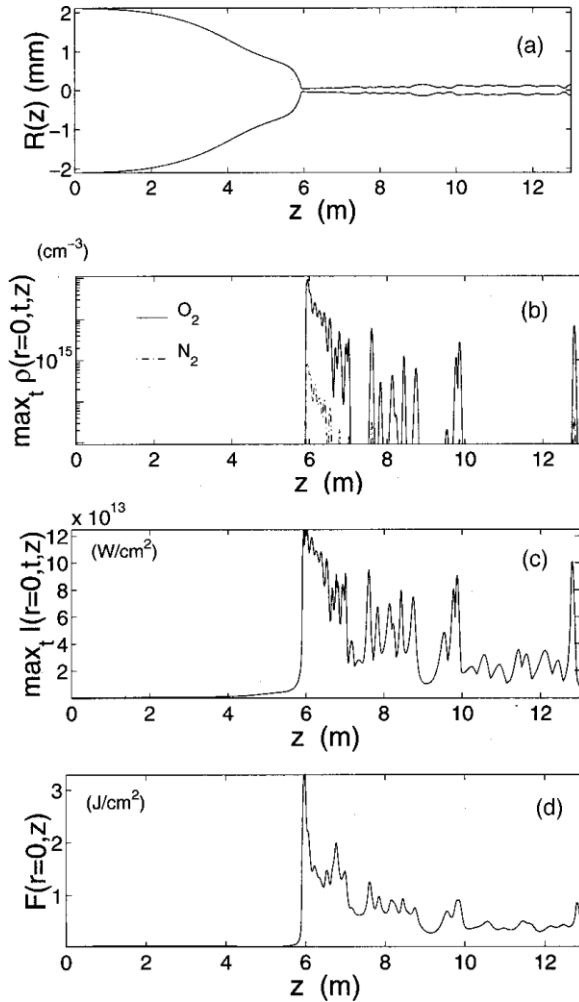


Figure 1.1 a) Mean radius, b) peak electron density, c) intensity, d) fluence of the filament core as a function of distance for a collimated input pulse at 800 nm with 5-mJ energy and 50 fs duration [2].

One can distinguish three stages of propagation. The first stage occurs in the absence of ionization and corresponds to the self-focusing regime. The second stage begins with the onset of ionization. It leads first to a continuous plasma column followed by quasi periodic cycles of focusing/defocusing due to competition between the optical Kerr effect and defocusing, and then by more intermittent focusing/defocusing cycle as the pulse power progressively decreases. Finally, in a third stage, not shown in the figure, the pulse power falls below P_{cr} . Bright light channels, stabilized by a competition between self-focusing and diffraction, propagate with little loss over long distances with a beam diameter increasing slowly [3]. The theoretical description of the filamentary propagation requires extensive simulations. Because of space-time coupling, there are no analytical solutions. Several reviews on the theory of filamentation are accessible

[4-6]. In this chapter, we briefly put the accent on some characteristic features of filaments before describing some possible applications.

1.2. Self-actions during filamentation

1.2.1. Filamentation is characterized by multiple self-actions

Beam self-stabilization: following beam collapse, the diameter of the beam becomes stable, as seen on a large scale $l \gg d$, where d is the average filament diameter. A microscopic inspection reveals a more complex behaviour, with the beam diameter slightly varying with distance due to the dynamic competition between Kerr self-focusing and plasma defocusing, as shown in Figure 1.1.

Pulse self-cleaning: the onset of ionization is accompanied by an improvement of the beam spatial profile, as seen in figure 1.2 [7-8]. At high incident peak powers $P \gg P_{cr}$, the beam splits into a multi-filament pattern. Here again, self-cleaning of the multi-filament pattern has been observed, as shown in Figure 1.3.

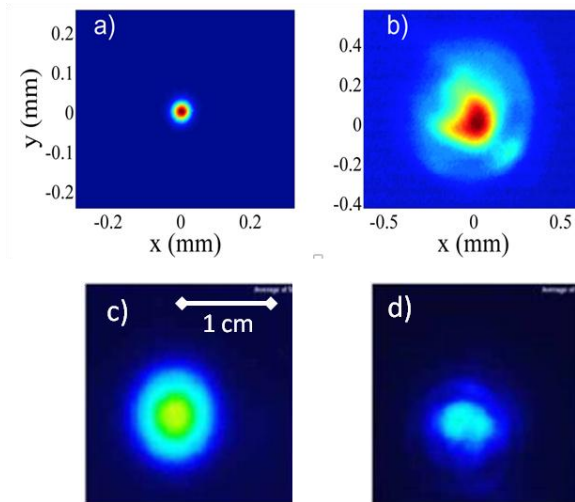


Figure 1.2 Beam profile in fused silica: after filamentation (a) and without filamentation (b) [9]. Beam profile measured in air 19 m from a fs laser at 800 nm: after filamentation (c) and without filament (d) [8].

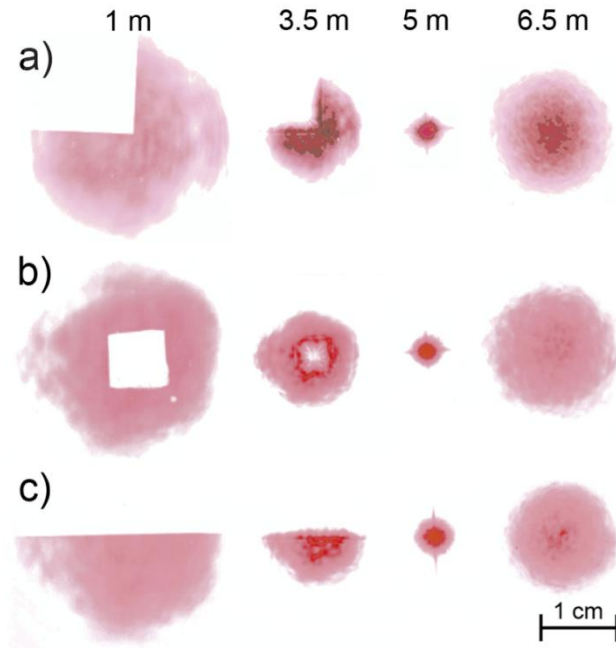


Figure 1.3 Burning patterns on photographic plates showing the beam profile of a 700 fs laser pulse with incident power $P \sim 10^2 P_{cr}$. The strongly distorted initial profile of the focused beam, recorded at different distances from the laser, exhibits near complete recovery of circular profile after focus (from ref [10]). A mask reduces the input laser energy by 25% in a), 10% in b) and 50% in c)

Self-frequency broadening: the rapid variation of the refractive index during the pulse and the ionization process lead to an important spectral broadening of the pulse. In air, the broadband continuum generated by a fs pulse at 800 nm covers the entire visible part of the spectrum [11].

Self-shortening of the pulse duration: the complex interactions occurring during beam collapse lead to successive pulse splitting and shortening, as shown in Figure 1.4 [12]. Extraction of the pulse at the right distance can yield pulses of duration close to the single cycle limit, as further discussed below in the applications section.

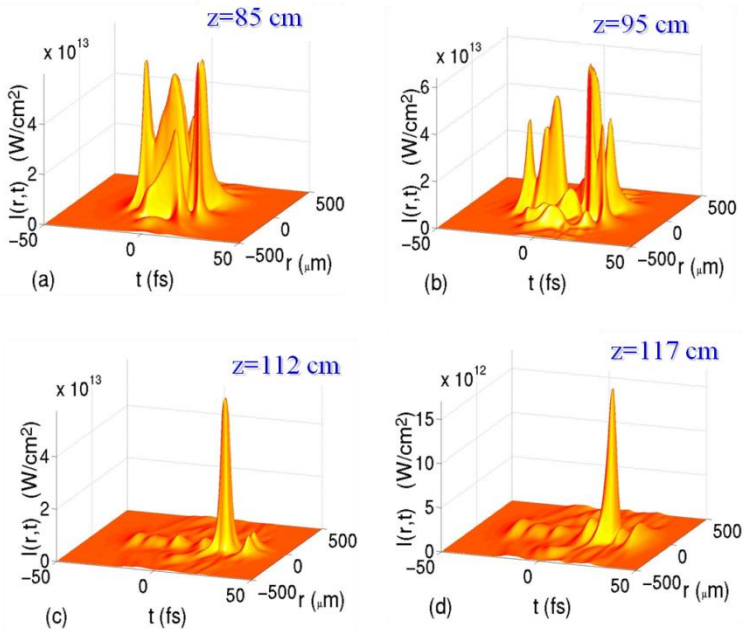


Figure 1.4 Calculated evolution of an initial converging femtosecond pulse with initial Gaussian profile upon propagation in Argon [12].

Group velocity dispersion: Group velocity dispersion plays an important role in filamentation. This can be understood by considering the role of the time-dependent change of refractive index during the pulse (see Figure 1.5). In the normal dispersion region, the ascending (descending) part of the pulse generates instantaneous frequencies on the redder (bluer) side of the pulse spectrum. Such frequencies separate from the pulse peak upon propagation if the system is in the normal dispersion region. By contrast, in the anomalous dispersion, the generated frequencies are sent back to the peak of the pulse, leading to pulse stabilization. As an example, Figure 1.6 compares the simulated propagation of a femtosecond laser pulse in the normal and anomalous dispersion region of fused silica. With a laser pulse at 800 nm (corresponding to the normal dispersion region), multiple pulse splitting and shortening is apparent. By contrast, a laser pulse of same incident peak intensity exhibits a smooth profile in the anomalous dispersion region. A self-guided pulse akin to a lossy spatio-temporal soliton emerges when $P \sim P_{cr}$ [9].

In recent years, several groups have started investigating short laser pulse propagation at mid IR wavelengths, where group velocity dispersion in air is low or even negative. The mechanism preventing beam collapse is different from the case of visible or near IR pulses. We refer to ref [13] and Vorolin and Zheltikov [14] for work in this domain.

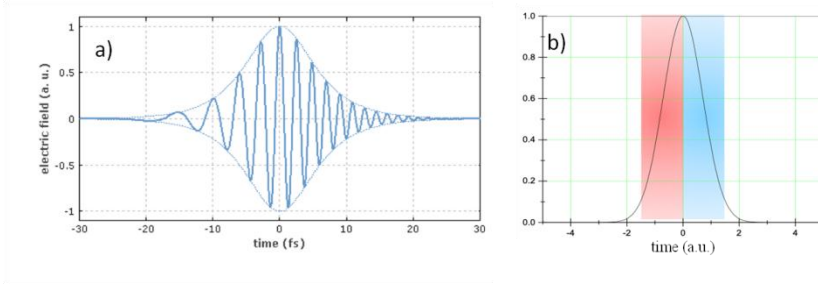


Figure 1.5 Self phase modulation shifts the spectrum in the front and the back of the pulse to the red and blue respectively.

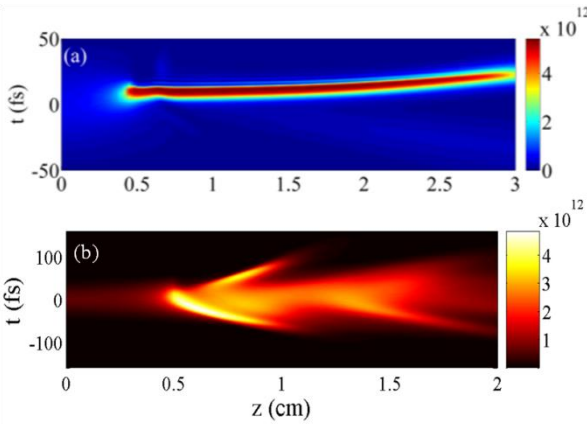


Figure 1.6 Numerical calculation of the pulse evolution during filamentation in silica for a femtosecond pulse with a central wavelength at $1.6 \mu\text{m}$ (a) and at 800 nm (b) [9].

Formation of low-density channels in air: Following beam collapse in air, part of the pulse energy is deposited in a long channel through Raman rotational excitation, ionization and inverse Bremsstrahlung [15]. This fast energy deposition is responsible for a sudden heating of air and the formation of a radially expanding cylindrical shockwave, leaving behind a central low-density channel with the same geometry as the filament, as shown in Figure 1.7 [16]. This under-dense channel then diffusively decays over a millisecond timescale, as shown in Figure 1.8.

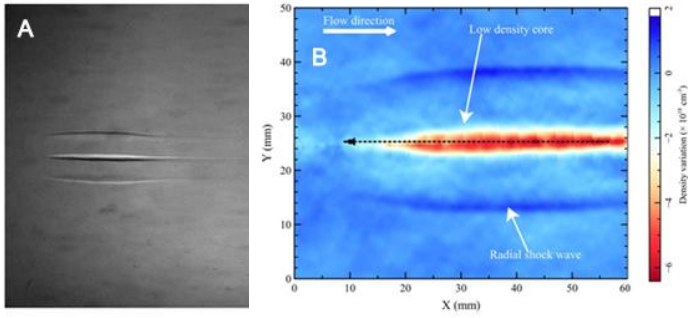


Figure 1.7 Image a low-density channel observed $6 \mu\text{s}$ after the filament formation in air. A) Schlieren image showing the radial shockwave. B) Density map obtained by interferometry [17].

The dynamics of the expanding shock wave and under-dense channel formation in air has been studied by means of transverse interferometry (see Figure 1.8) [17-18]. In the case of relatively tight focusing ($f/35$), channels with a density decrease of more than 60 % are observed, lasting for more than 90 ms.

Such long-lived hydrodynamic structures have been used to create remote virtual waveguides in air [19-20]. By placing several filaments in a square or circle, one obtains an increased air density region in the centre of the configuration, the over-density of which can act as a long-lasting waveguide for lasers at other wavelengths, as demonstrated by the Milchberg group at the University of Maryland [19].

Filamentation-induced low-density channels in air also play an important role in the triggering and guiding of electric discharges [21-22] and for aerodynamic control [17], as discussed below.

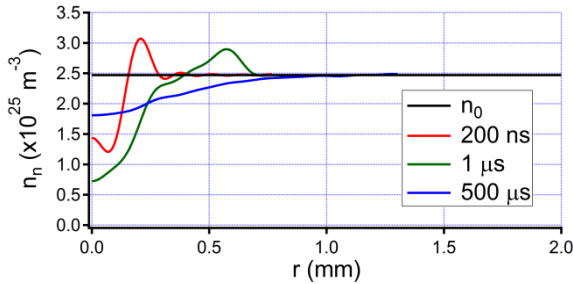


Figure 1.8 Measured evolution of air density after formation of a filament [18].

1.3. Applications

1.3.1. Spatio-temporal femtosecond laser pulse improvement

For many ultrafast applications, it is important to start with a short laser pulse of high quality. Of particular importance is a smooth spatial profile and the absence of pulse precursor. One can exploit the self-cleaning action of filaments to improve

the quality of a femtosecond laser pulse. The scheme is shown in Figure 1.9a. A fs pulse with strongly distorted beam profile and with significant pre-pulse energy is incident on two counterpropagating filaments. The retro reflected pulse displays considerable improvement in the beam profile. Also, pre-pulse energy is removed (see figures 1.9b and 1.9c) [23].

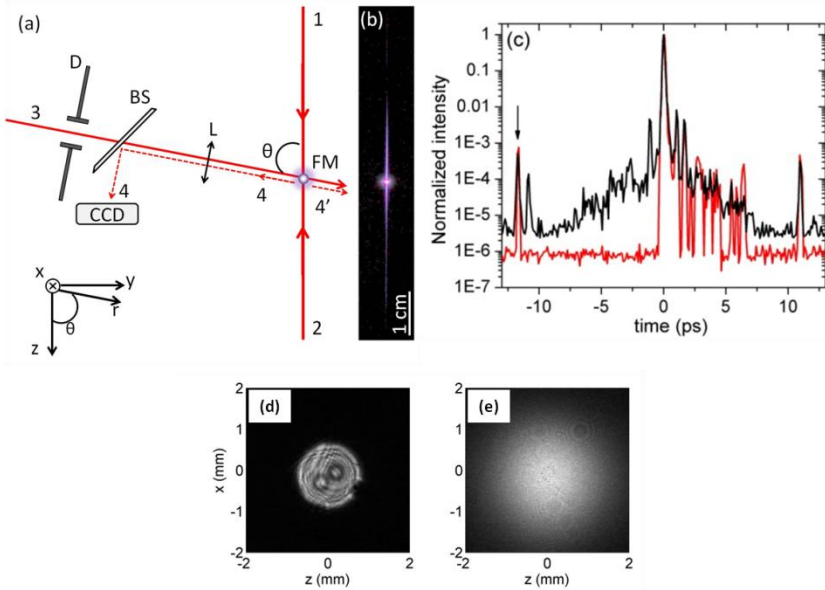


Figure 1.9 (a) Schematic set-up. Pulses 1,2 and 3 are time coincident at point of intersection. D: diaphragm; BS: beam splitter; L: lens; CCD: charge coupled device camera; FM: filament mirror; (b) Photograph of the plasma luminescence from the two counterpropagating filaments forming the mirror. (c) Temporal contrast of the probe (in black) and of the reflected beam (red) measured with a third order cross correlator. Fluence profile of a probe femtosecond pulse with strongly distorted spatial profile before (d) and after retro-reflection on the filament mirror (e).

1.3.2. Temporal pulse improvement

There are strong incentives to obtain laser pulses with duration close to the fundamental limit of one optical cycle. Such short pulses are essential for XUV attosecond pulse generation, for ultrafast streaking physics and may reduce the costs to reach the ultra-relativistic intensity regime, since the cost of amplifiers scales with pulse energy. One can exploit the property of filaments to reduce the duration of the propagating pulse close to the single cycle limit. Figure 1.10 shows the experimental setup used by U. Keller group in Zurich to demonstrate this effect [24]. Filamentation occurs in two successive Argon cells, with optimized pressure. Figure 1.11 shows the pulse duration measured after each cell [25].

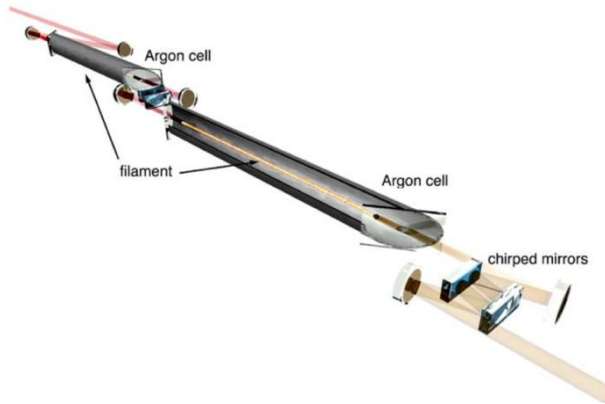


Figure 1.10 Experimental set up for the shortening of fs pulses via double filamentation in Argon [24].

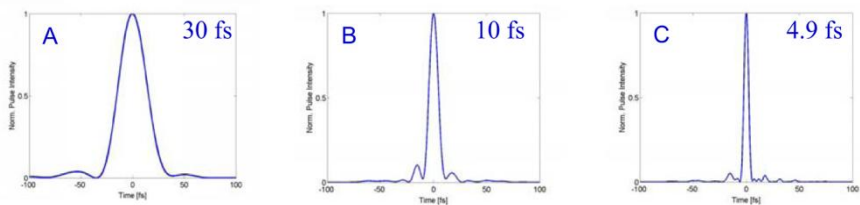


Figure 1.11 Pulse duration at a) input of first filament stage, b) after first filament stage, c) after second filament stage (from ref. 25).

1.3.3. Triggering and guiding of electric discharges

Plasma filaments can be particularly useful for the remote manipulation of high voltage discharges. They can trigger and guide megavolts discharges in air over several meters [26-27], carry high DC currents with reduced losses [28] or deviate arcs from their natural path [22]. These properties are of great interest for applications such as the laser lightning rod [29-30], virtual plasma antennas for radiofrequency transmission [31] or high voltage switch [32].

The physical mechanism is the following. As discussed in the previous part, laser energy deposition in the filament leads to the appearance of a hot, low density channel at the center of the filament path. In addition, a fraction of the free electrons produced by the laser pulse does not recombine on the parent ions but becomes attached to neutral oxygen molecules. These loosely bound electrons can be easily released by current heating, leading to a decrease of the leader inception voltage [33]. This offers a privileged path for electric discharges [21,34]. A filament decreases the breakdown voltage in a gas by more than 30% and guides the discharge over the perfectly straight path defined by the laser. See Figure 1.12 Recently, a european funded project has been started with the aim to exploit this effect for implementing an active lightning rod. For more details see ref [30].

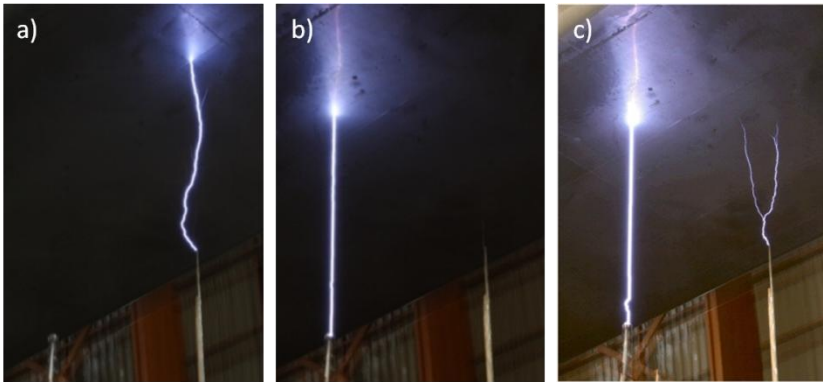


Figure 1.12 Diversion action of a filament on electric discharges. (a) A spontaneous discharge always originates at the sharp grounded electrode on the right. (b-c) With a filament, the guided discharge originates always at a rounded ground electrode located further apart from the HV electrode plate [from ref. 22].

Fast high voltage triggers: Classical high voltage triggering switches based on electronics and avalanche breakdown present a jitter (defined as the standard deviation of the switching time delay) in the sub-microsecond range. This jitter is a severe limitation for multi-stages high voltage generator and for applications where high voltage pulses have to be precisely synchronized [32].

Since laser filaments decrease the breakdown voltage of a spark gap in a very fast and reproducible way, they also reduce significantly the jitter of an air switch, which is on the order of 0.2 ns, as shown in Figure 1.13.

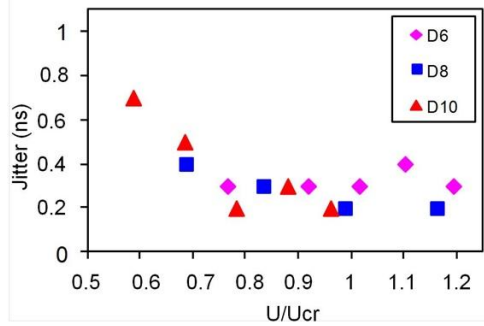


Figure 1.13 Jitter of the switch as a function of normalized voltage for inter-electrode gaps of 6, 8 and 10 mm [32].

In addition, the long and uniform plasma channels formed by the filament offer the possibility to trigger simultaneously several air spark gaps with an excellent synchronization. This effect has been used to build a multi-stage Marx generator triggered in atmospheric air by a single filament. The generator is composed of 6 stages connected by 5 gap switches similar to the one presented in the previous section. Every stage includes six capacitors of 2 nF connected in parallel par metal plates and charged up to 27 kV (slightly below self-breakdown). The two electrodes on each gap switch are pierced on the axis with a hole of 3 to 4.5 mm in diameter and separated by 11 mm. When a beam of multiple filaments is formed inside the generator, all stages of the generator are connected simultaneously and a voltage pulse of 160 kV is generated at the output of the generator. This voltage pulse has a rise time of a few nanoseconds and a sub-nanosecond jitter, as shown in Figure 1.14 [35].

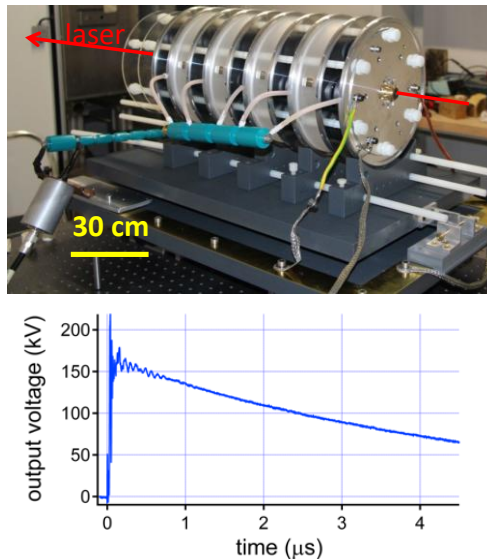


Figure 1.14 High voltage Marx generator fully triggered by a single filament. Voltage rise-time of 5 ns for a voltage pulse of 160 kV.

1.3.4. Improving transport

1.3.4.1. Improving the speed of trains

The contact between pantograph and power line sets a limit to the speed of fast trains, because of the mechanical friction and the generation of unwanted oscillations in the powerline at high speeds. Experiments performed at the test site of TGV trains in France have shown that this difficulty could in principle be overcome by connecting the current collecting pantograph to the power supply line via cm long electric discharges induced by filamentation [28]. A contactless connection proved efficient for both DC and AC power supply, transmitting an electric power in the MW range with little power loss, amounting to 1-2 % (see Figure 1.15).

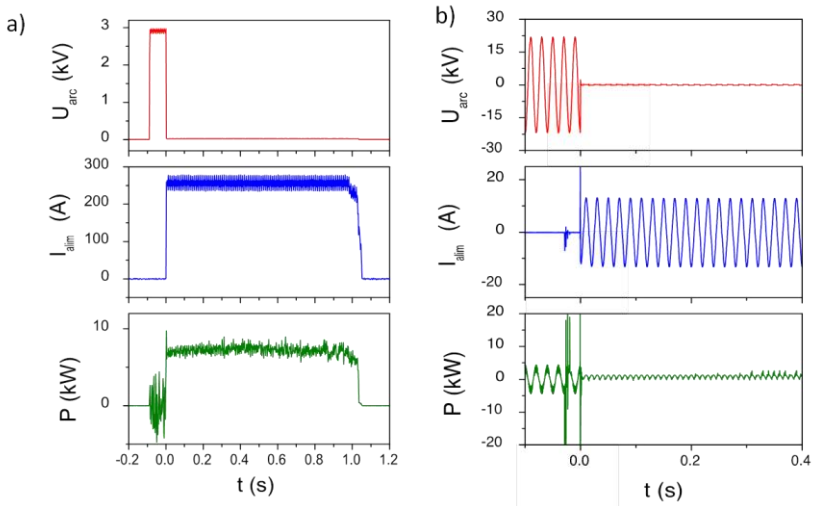


Figure 1.15 Filament induced power supply. (a) DC power coupling. (b) AC power coupling. The arrival of the laser pulse at $t = 0$ leads to a rapid drop of the voltage of the charged electrode and to a surge of the current. The lower trace shows the power dissipated in the discharge.

1.3.4.2. Improving supersonic flights

When a vehicle moves in atmosphere at supersonic velocity, a shock wave is generated, leading to a considerable increase of the drag experienced by the vehicle and of its fuel consumption. A common strategy to reduce the drag is to give a slender shape to the front of the vehicle, in the form of a spike. Mechanical instabilities and manoeuvrability constraints put a limit to this approach. Several authors have suggested that depositing an immaterial plasma spike could circumvent these limitations.

Experimental tests performed in the supersonic wind tunnel of ONERA in Meudon, France with a mobile TW laser showed that filamentation led to a significant reduction of the drag experienced by a blunt test model [17]. The filament induced by a fs laser pulse emerging from the nose of the test model led to a low-density channel that perturbed the conical wave, with a transient reduction by

50 % of the drag experienced by the test model at Mach 3. It was also shown that weightless manoeuvrability can be achieved by a slight displacement of the beam direction from the module axis.

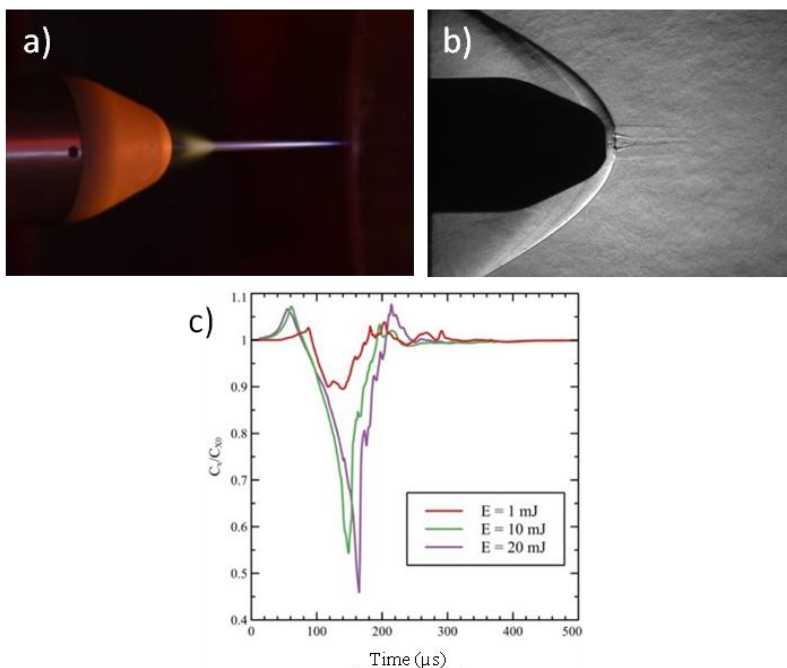


Figure 1.16 (a) Still photography of the filament produced in front of the blunt body. (b) Schlieren image showing the shockwave at Mach 3 and its perturbation by the filament in the presence of the Mach3 airflow [17]. (c) Normalized drag signal measured on the model after the formation of the filament for 3 different laser energies.

1.3.5. Virtual plasma antenna

There are incentives to replace conventional antennas by virtual antennas where plasma replaces metal. Such antennas could be broadband, easily reconfigurable, easily deactivated, stealthy and would lead to a reduction of co-site interference between multiple adjacent antennas [36]. Most designs so far use low-pressure plasmas confined inside solid dielectric vessels. Recently, a new concept based on filament guided electric discharges has been demonstrated [31,37]. This virtual plasma antenna is tuneable in a large frequency range (100 MHz – 1 GHz).

Figure 1.17a shows a proof of principle implementation. A meter-scale conductive plasma column is formed in air by guiding an electric discharge generated by a compact Tesla coil (output voltage of 350 kV) using an ultrashort laser pulse (700 fs, 300 mJ @ 800 nm) undergoing filamentation. Radio-frequency (RF) power is then injected in the plasma by means of an inductive coupler. Radio emission was detected with a remote patch antenna of 100 MHz - 1 GHz bandwidth (Figure 1.17b).

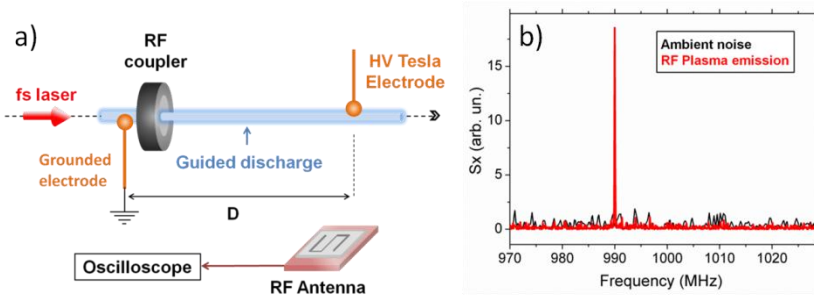


Figure 1.17(a) Experimental setup used for RF coupling in the plasma. (b) Emitted RF signal strength with (red) or without (black) the plasma column when the coupler is excited at 990 MHz.

In the first demonstration experiment of Brelet *et al.*, the duration of the emission was limited by the lifetime of the discharge to 100 ns. Techniques to increase the lifetime of the plasma antenna have been since developed. The idea is to inject a long lived current from a secondary source in the guided discharge. An increase of the plasma lifetime to the millisecond regime has been demonstrated [38-39].

1.3.6. Remote production of secondary radiation sources

The remote production of filaments in air leads to the production of coherent and directed secondary radiation sources, ranging from THz to UV.

1.3.6.1. Filament induced coherent terahertz radiation in air

Because of the Lorentz force, the plasma created during filamentation in air is left with a longitudinal oscillation, heavily damped by collisions. This moving plasma column acts as a progressive antenna and gives rise to a forward oriented conical emission of short bursts of THz radiation, as shown in Figure 1.18 [40].

Although the conversion efficiency is low, on the order of 10^{-9} , this THz source has several advantages. Since filaments can be deposited at km distance from the laser source [41], it leads to the possibility to remotely create a short THz pulse close to a distant target, avoiding the problem of THz wave attenuation by air humidity. Also, since there is no material other than air for THz production, there is no risk of damage limiting the initial laser power. The THz intensity is then expected to increase by a factor $N \sim P/P_{cr}$. This was confirmed with a laser of 2 TW peak power (producing around 20 filaments), where an increase of THz signal by a factor 20 as compared to a single filament was observed at a distance of 20 m from the laser (see Figure 1.19) [42]. Even more interesting, it was shown that it is possible to interfere constructively the THz emission from separate filaments [43]). With proper organization of filaments in the form of a phased array, directionality and an increase of the THz intensity scaling like N^2 is expected.

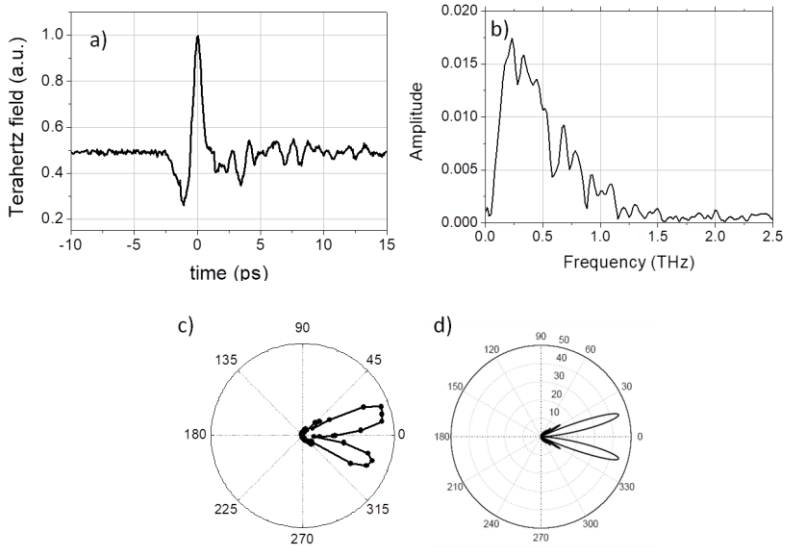


Figure 1.18 (a) Temporal shape of the THz field emitted by a single filament measured by electro-optic sampling in ZnTe crystal and (b) corresponding spectrum obtained by Fourier transform. (c) Angular distribution of the THz emission measured at 0.1 THz and (d) calculated using the transition Cerenkov model of ref [40].

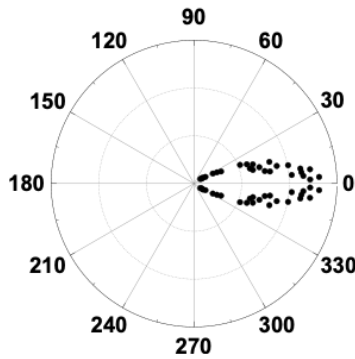


Figure 1.19 Angular distribution of the THz from filaments generated in air by a terawatt laser beam [42].

1.3.6.2. Filament induced coherent UV emission in air

The plasma column created in air during filamentation of a fs laser pulse at 800 nm can act as an amplifying medium for UV radiation. Stimulated amplification of an injected seed at 337, 391 and 428 nm, has been observed from nitrogen molecules following filamentation with a femtosecond pump laser pulse at 800 nm [44-45]. Figure 1.20 shows the energy level structure of N_2 and N_2^+ and the corresponding

laser transitions. Amplification at 337 nm takes place if the pump pulse is circularly polarized but disappears with linearly polarized pump light while a reverse polarization dependence is observed for the two other wavelengths. While the origin of amplification of lines at 391 and 428 nm is still controversial, the excitation mechanism for the 337 nm emission is well understood: the energy distribution of free electrons generated by the circularly polarized pump pulse at 800 nm has an initial peak at $2U_p$, where $U_p = e^2 I / 2c\epsilon_0 m\omega^2$ is the free electron ponderomotive energy. For a laser peak intensity of $1.5 \cdot 10^{14} \text{ W/cm}^2$ this corresponds to 14 eV, sufficient to excite neutral molecules from ground level $X^1\Sigma_g^+$ of the neutral molecule to excited level $C^3\Pi_u^+$ by multiple electron-neutral molecule collisions, producing a transient inversion of population between levels $C^3\Pi_u^+$ and $B^3\Pi_g^+$ [46]. A dream of atmosphere scientists is to have a lasing signal in air propagating backwards, towards the pump source, since it would considerably increase the signal detection efficiency. Interestingly, the 337 nm amplified emission has also been observed in the backward directions with respect to the pump pulse direction, as shown in figure 1.21. Unfortunately, oxygen acts as a quenching mechanism, preventing so far the observation of significant backward stimulated emission in air with oxygen concentration exceeding 10% [47].

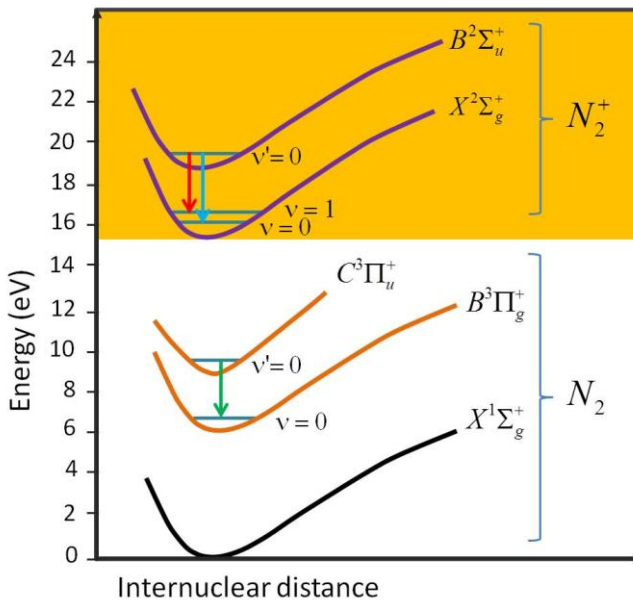


Figure 1.20 Energy level structure of N_2 and N_2^+ and the corresponding laser transitions.

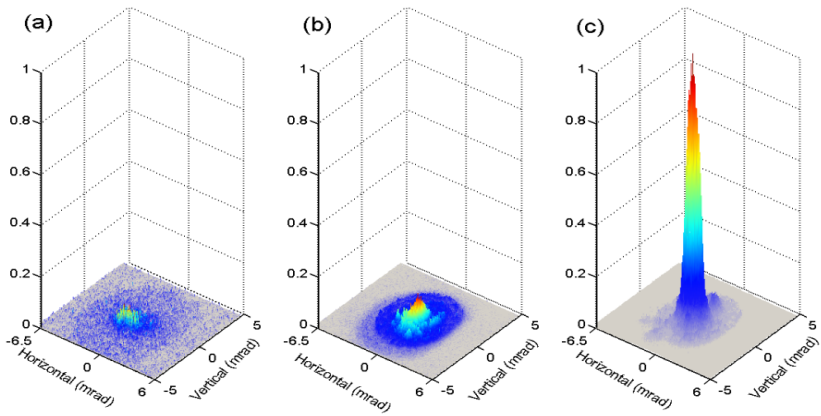


Figure 1.21 Spatial profile of the backward ASE (a), the seed pulse (b), and the backward amplified 337 nm radiation (c) in nitrogen [46].

1.4. Conclusion

In this chapter, we have briefly described several properties of filaments and their potential use in applications. The list of presented items is far from being exhaustive. Many applications can be seen as futuristic. Their viability will depend on the development of reliable femtosecond laser sources.

Acknowledgments

This work has been partially supported by DGA (Délégation Générale à l'Armement), France

References

1. Marburger J. H. 'Self-focusing: Theory'. *Progress in Quantum Electronics* 1975;**4**: 35-110
2. Couairon A. Tzortzakis S. Bergé L. Franco M. Prade B. Mysyrowicz A. 'Infrared femtosecond light filaments in air: simulations and experiments'. *J. Opt. Soc. Am. B* 2002;**19**: 1117-1131
3. Mechain G. et al., 'Long-range self-channeling of infrared laser pulses in air: a new propagation regime without ionization'. *Applied Physics B* 2004 ;**79** : 379–382
4. Couairon A. Mysyrowicz A., 'Femtosecond filamentation in transparent media'. *Physics Reports* 2007;**441**(2) pp. 47-189
5. Chin S L Hosseini S A Liu W Luo Q Théberge F Aközbeq N Becker A Kandidov V P Kosareva O G Schroeder H. 'The propagation of powerful femtosecond laser pulses in optical media: physics, applications, and new challenges.' *Canadian Journal of Physics* 2005;**83**(9): 863-905
6. Kolesik M. Moloney J. V. 'Modeling and simulation techniques in extreme nonlinear optics of gaseous and condensed media'. *Reports on Progress in Physics* 2014;**77**(1): 016401
7. Moll K. D. Gaeta A. L. Fibich G. 'Self-Similar Optical Wave Collapse: Observation of the Townes Profile'. *Physical Review Letters* 2003;**90**: 203902
8. Prade B. Franco M. Mysyrowicz A. Couairon A. Buersing H. Eberle B. Krenz M. Seiffer D. Vasseur O. 'Spatial mode cleaning by femtosecond filamentation in air'. *Optics Letters* 2006;**31**: 2601-2603
9. Durand M. Jarnac A. Houard A. Liu Y. Grabielle S. Forget N. Durécu A. Couairon A. Mysyrowicz A. 'Self-guided propagation of ultrashort laser pulses in the anomalous dispersion region of transparent solids: a new regime of filamentation'. *Physical Review Letters* 2013;**110**: 115003
10. Milian C., Jukna V. Couairon A. Houard A. Forestier B. Carbonnel J. Liu Y. Prade B. Mysyrowicz A. "Laser beam self-symmetrization in air in the multifilamentation regime". *Journal of Physics B* 2015;**48**: 094013
11. Kasparian J. Sauerbrey R. Mondelain D. Niedermeier S. Yu J. Wolf J.-P. André Y.-B. Franco M. Prade B. Tzortzakis S. Mysyrowicz A. Rodriguez M. Wille H. Wöste L. 'Infrared extension of the supercontinuum generated by femtosecond terawatt laser pulses propagating in the atmosphere'. *Optics Letters* 2000;**25**: 1397-1399
12. Couairon A. Biegert J. Hauri C. P. Kornelis W. Helbing F. W. Keller U. Mysyrowicz A. 'Self-compression of ultra-short laser pulses down to one optical cycle by filamentation'. *Journal of Modern Optics* 2006;**53**(1-2): 75-85
13. Panagiotopoulos P. Whalen P. Kolesik M. et al. 'Super high power mid-infrared femtosecond light bullet'. *Nature Photonics* 2015;**9**: 543–548
14. Voronin A. A. Zheltikov A. M. 'Long-wavelength infrared solitons in air'. *Optics Letters* 2017;**42**: 3614-3617
15. Cheng Y.-H. Wahlstrand J. K. Jhajj N. and Milchberg H. M. *Optics Express* 2013;**21**, 4740
16. Wahlstrand J. K. Jhajj N. Rosenthal E. W. Zahedpour S. and Milchberg H. M. 'Direct imaging of the acoustic waves generated by femtosecond filaments in air'. *Optics Letters* 2014;**39**: 1290
17. Elias P.-Q. Severac N. Luyssen J.-M. André Y.-B. Doudet I. Wattellier B. Tobeli J.-P. Albert S. Mahieu B. Bur R. Mysyrowicz A. Houard A. 'Improving

- supersonic flights with femtosecond laser filamentation'. *Science Advances* 2018;**4**: eaau5239
18. Point G. Milián C. Couairon A. Mysyrowicz A. and Houard A. 'Generation of long-lived underdense channels using femtosecond filamentation in air'. *Journal of Physics B* 2015;**48**: 094009
 19. Jhaji N. Rosenthal E. Birnbaum R. Wahlstrand J. Milchberg H. M., 'Demonstration of long-lived high power optical waveguides in air'. *Physical Review X* 2014;**4**: 011027
 20. Lahav O. Levi L. Orr I. Nemirovsky R. A. Nemirovsky J. Kaminer I. Segev M. Cohen O. 'Long-lived waveguides and sound-wave generation by laser filamentation'. *Physical Review A* 2014;**90**: 021801
 21. Tzortzakis S. Prade B. Franco M. Mysyrowicz A. Hüller S. and Mora P. 'Femtosecond Laser-guided Electric Discharge in Air'. *Physical Review E* 2001;**64**: 57401
 22. Forestier B. Houard A. Revel I. Durand M. André Y. B. Prade B. Jarnac A. Carbonnel J. Le Nevé M. de Miscault J. C. Esmiller B. Chapuis D. and Mysyrowicz A. 'Triggering, guiding and deviation of long air spark discharges with femtosecond laser filament'. *AIP Advances* 2012;**2**: 012151
 23. Jarnac A. Durand M. Houard A. Liu Y. Prade B. Richardson M. Mysyrowicz A. 'Spatiotemporal cleaning of a femtosecond laser pulse through interaction with counterpropagating filaments in air'. *Physical Review A* 2014;**89**: 023844
 24. Hauri C. P. Kornelis W. Helbing F. W. Couairon A. Mysyrowicz A. Biegert J. and Keller U. 'Generation of intense, carrier-envelope phase-locked few-cycle laser pulses through filamentation'. *Applied Physics B* 2004;**79**: 673
 25. Zaïr A. Guandalini A. Schapper F. Holler M. Biegert J. Gallmann L. Keller U. Couairon A. Franco M. Mysyrowicz A. 'Spatio-temporal characterization of few-cycle pulses obtained by filamentation'. *Optics Express* 2007;**15**: 5394
 26. Pépin H. Comtois D. Vidal F. Chien C. Y. Desparois A. Johnston T. W. Kieffer J. C. La Fontaine B. Martin F. Rizk F. A. M. 'Triggering and guiding high-voltage large-scale leader discharges with sub-joule ultrashort laser pulses'. *Physics of Plasmas* 2001;**8**: 2532
 27. Rodriguez M *et al.* 'Triggering and guiding megavolt discharges by use of laser-induced ionized filaments'. *Optics Letters* 2002;**27**: 772
 28. Houard A. D'Amico C. Liu Y. André Y. B. Franco M. Prade B. Salmon E. Pierlot P. Cléon L.-M. Mysyrowicz A. 'High Current Permanent Discharges in Air Induced by Femtosecond Laser Filamentation'. *Applied Physics Letters* 2007;**90**: 171501
 29. Zhao X. M. Diels J.-C. Braun A. Liu X. Du D. Korn G. Mourou G. Elizondo J. M. 'Use of self-trapped filaments in air to trigger lightning' in *Ultrafast Phenomena*, Springer Series in Chemical Physics. New York: Springer-Verlag 1994;**60**: 233
 30. Produit T. Walch P. Herkommer C. Mostajabi A. Moret M. Andral U. Sunjerga A. Azadifar M. André Y.-B. Mahieu B. Haas W. Esmiller B. Fournier G. Krötz P. Metzger T. Michel K. Mysyrowicz A. Rubinstein M. Rachidi F. Kasparian J. Wolf J.-P. Houard A. 'The Laser Lightning Rod project'. *The European Physical Journal: Applied Physics* 2020;**92**, 30501
 31. Brelet Y. Houard A. Point, G. Prade, B. Arantchouk L. Carbonnel J. Andre Y.-B. Pellet M. Mysyrowicz A. 'Radiofrequency plasma antenna generated by femtosecond laser filaments in air'. *Applied Physics Letters*. 2012;**101**: 264106

32. Arantchouk A. Houard A. Brelet Y. Carbonnel J. Larour J. André Y.-B. Mysyrowicz A. 'A simple high-voltage high current spark gap with subnanosecond jitter triggered by femtosecond laser filamentation'. *Applied Physics Letters*. 2013;**102**: 163502
33. Comtois D. et al. 'Triggering and Guiding of an Upward Positive Leader From a Ground Rod With an Ultrashort Laser Pulse—II: Modeling'. *IEEE Trans. on Plasma Science* 2003;**31**: 387
34. Vidal F. et al. Modeling the triggering of streamers in Air by ultrashort laser pulses *IEEE Trans. on Plasma Science* 2000;**28**: 418
35. Arantchouk A. Point G. Brelet Y. Larour J. Carbonnel J. André Y.-B. Mysyrowicz A. Houard A. 'Compact 180-kV Marx generator triggered in atmospheric air by femtosecond laser filaments'. *Applied Physics Letters*. 2014;**104**: 103506
36. Borg G. G. Harris J. H. Martin N. M. Thorncraft D. Milliken R. Miljak D. G. Kwan B. Ng. T. and Kircher J. 'Plasmas as antennas: Theory, experiment and applications'. *Physics Plasmas*. 2000;**7**: 2198
37. Théberge F. Gravel J.-F. Kieffer J.-C. Vidal F. Châteauneuf M. 'Broadband and long lifetime plasma-antenna in air initiated by laser-guided discharge'. *Applied Physics Letters* 2017;**111**: 073501
38. Arantchouk L. Honnorat B. Thouin E. Point, G. Mysyrowicz A. Houard A. 'Prolongation of the lifetime of guided discharges triggered in atmospheric air by femtosecond laser filaments up to 130 μ s'. *Applied Physics Letters*. 2016;**108**: 173501
39. Théberge, F. Daigle JF. Kieffer, JC et al. 'Laser-guided energetic discharges over large air gaps by electric-field enhanced plasma filaments'. *Scientific Report* 2017;**7**: 40063 (2017)
40. D'Amico C. Houard A. Franco M. Prade B. Couairon A. Tikhonchuk V.T. Mysyrowicz A. 'Conical forward THz emission from femtosecond laser filamentation in air'. *Physical Review Letters* 2007;**98**: 235002
41. Durand M. Houard A. Prade B. Mysyrowicz A. Durécu A. Moreau B. Fleury D., Vasseur O. Borchert H. Diener K. Schmitt R. Théberge F. Chateauneuf M., Daigle J.-F and Dubois J. 'Kilometer range filamentation'. *Optics Express* 2012;**21**: 26836
42. D'Amico C. Houard A. Akturk S., Liu Y. Le Bloas J. Franco M. Prade B. Couairon A. Tikhonchuk V.T. Mysyrowicz A. 'Forward THz radiation emission by femtosecond filamentation in gases: theory and experiment'. *New Journal of Physics* 2008;**10**: 013015
43. Mitryukovskiy S. I. Liu Y. Prade B. Houard A. and Mysyrowicz A. 'Coherent interaction between the THz radiation emitted by filaments in air'. *Laser Physics* 2014;**24**: 094009
44. Liu Y. Ding P. Lambert G. Houard A. Tikhonchuk V. T. Mysyrowicz A. 'Recollision-induced superradiance of ionized nitrogen molecule'. *Physical Review Letters* 2015;**115**: 133203
45. Yao J. Jiang S. Chu W. Zeng B. Wu C. Lu R. Li Z. Xie H. Li G. Yu C. Wang Z., Jiang H. Gong Q. and Cheng Y. 'Population redistribution among multiple electronic states of molecular nitrogen ions in strong laser fields'. *Physical Review Letters* 2016;**116**: 143007
46. Ding P. Oliva E. Houard A. Mysyrowicz A. Liu Y. 'Lasing dynamics of neutral nitrogen molecules in femtosecond filaments'. *Physical Review A* 2016;**94**: 043824

47. Gui J. Zhou D. Zhang X. Lu Q. Luo Y. Liang Q. Danylo R. Houard A. Mysyrowicz A. Liu Y. 'Quenching Effect of O₂ on Cavity-free Lasing of N₂ Pumped by Femtosecond Laser Pulses'. *Acta Photonica Sinica* 2020;**49**: 1149013